Mössbauer studies of the non-heme iron and cytochrome b_{559} in a *Chlamydomonas reinhardtii* PSI$^-$ mutant and their interactions with α-tocopherol quinone

Květoslava Burda[a], Jerzy Kruk[b], Rüdiger Borgstädt[c], Jan Stanek[d], Kazimierz Strzałka[b], Georg H. Schmid[c], Olaf Kruse[c,*]

[a] *Institute of Nuclear Physics, ul. Radzikowskiego 152, 31-342 Cracow, Poland*
[b] *Faculty of Biotechnology, Jagiellonian University, al. Mickiewicza 3, 31-120 Cracow, Poland*
[c] *Lehrstuhl Zellphysiologie, Fakultät für Biologie, Universität Bielefeld, Postfach 10 01 31, D-33501 Bielefeld, Germany*
[d] *Institute of Physics, Jagiellonian University, ul. Reymonta 4, 31-059 Cracow, Poland*

Received 20 September 2002; revised 13 December 2002; accepted 13 December 2002

First published online 9 January 2003

Edited by Richard Cogdell

Abstract **Spin and valence states of the non-heme iron and the heme iron of cytochrome b_{559}, as well as their interactions with α-tocopherol quinone (α-TQ) in photosystem II (PSII) thylakoid membranes prepared from the *Chlamydomonas reinhardtii* PSI$^-$ mutant have been studied using Mössbauer spectroscopy. Both of the iron atoms are in low spin ferrous states. The Debye temperature of the non-heme is 194 K and of the heme iron is 182 K. The treatment of α-TQ does not change the spin and the valence states of the non-heme iron but enhances the covalence of its bonds. α-TQ oxidizes the heme iron into the high spin Fe^{3+} state. A possible role of the non-heme iron and α-TQ in electron flow through the PSII is discussed.**

Key words: Photosystem II; Non-heme iron; Cytochrome b_{559}; α-Tocopherol quinone

1. Introduction

There are many redox cofactors participating in the photosynthetic electron transport chain within photosystem II (PSII) [1]. The primary electron acceptor pheophytin receives an electron from the excited reaction center chlorophyll *a* species P680*, transferring it to the bound plastoquinone, Q_A. Then the electron is transferred from the reduced Q_A^- to a second plastoquinone, Q_B. In two turnovers Q_B, which has accepted two electrons and taken up two protons, is replaced by a new oxidized plastoquinone. Molecule $P680^+$ is reduced by the primary donor tyrosine-161 Y_z. The water oxidizing complex extracts electrons from H_2O transferring it to Y_z.

The tertiary structure of PSII is presently known to be of 3.8 Å resolution [2] but the action of some of its redox components is not known. For example, the action of cytochrome b_{559}, which has no counterpart in the bacterial photosynthetic reaction center, has not yet been explained [3,4]. Participation of cytochrome b_{559} in the cyclic electron transport or in a side path of electron flow through PSII has been suggested as a protection against photoinhibition [5]. Its role in stabilization of oxygen evolution during photoactivation and/or as a proton acceptor during the S-state turnover has been discussed [6–8], as well as its action as scavenger of photogenerated free radicals [9]. Cytochrome b_{559} is a heterodimer containing two subunits, α and β connected through heme. The heme is located on the stromal side of the membrane about 28 Å apart from the plastoquinone Q_B site [2,10]. The available sequences show highly conserved transmembrane segments of the α and β proteins and predict one histidine residue on each of the subunits [11,12]. The spectroscopic analysis indicates that the heme iron is ligated in its fifth and sixth coordination positions by histidine nitrogens. Independently of its valence state (ferric or ferrous) it was found to be in low spin state [13,14]. Cytochrome b_{559} has an unusually high and variable midpoint reduction potential. It occurs mainly in two potential forms, a high potential (HP; $E_{m,7} = 350$–400 mV) and a low potential form (LP; $E_{m,7} = 0$–80 mV) in thylakoids [4] but also other potential forms were described, like intermediate potential (IP; $E_{m,7} = 150$–270 mV) [15,16] and the very low potential form (VLP; $E_{m,7} = -45$ mV) [17]. The function of cytochrome b_{559} is probably associated with the conversion between its HP ↔ LP form. However, the mechanism of the switch between these two potential forms is not recognized yet. Cytochrome b_{559} was shown to undergo redox reactions in the presence of membrane prenylquinones [18], which can be associated with its photoprotective function. Especially, the interaction of α-tocopherol quinone (α-TQ) with the cytochrome seems to be interesting in this respect, because it was shown that this prenylquinone quenches effectively PSII fluorescence by a mechanism similar to that of carbonylcyanide-*p*-trifluoromethoxy-phenyl-hydrazone (FCCP), i.e. by deprotonation of the HP form of cytochrome b_{559} [19,20] causing oxidation of this cytochrome b_{559} form. It was also shown that α-TQ is able to oxidize directly the LP form of cytochrome b_{559} [18].

Another intriguing component is the non-heme iron located between Q_A and Q_B sites (about 7 Å from each of them) [2,21,22]. Non-heme iron is probably coordinated by four his-

*Corresponding author. Fax: (49)-521-106 64 10.
E-mail address: olaf.kruse@biologie.uni-bielefeld.de (O. Kruse).

Abbreviations: α-TQ, α-tocopherol quinone; FCCP, carbonylcyanide-*p*-trifluoromethoxy-phenyl-hydrazone; δ, isomer shift; Δ*E*, quadrupole splitting; HP, high potential; LP, low potential

0014-5793/03/$22.00
doi:10.1016/S0014-5793(02)03895-4

tidine residues and glutamate in anoxygenic purple bacteria [23]. The four histidines from the bacterial reaction center are conserved in green algae and higher plants with the exception that the glutamate ligand might be replaced by bicarbonate [24]. In addition, the non-heme iron has been shown, unlike the bacterial reaction center homologue, to undergo redox changes of Fe^{2+}/Fe^{3+} [25]. Usually, in the reaction center of purple bacteria [22], as well as in PSII from algae and higher plants [26,27], non-heme iron appears in a reduced high spin state Fe^{2+}. It can be oxidized by ferricyanide to the high spin Fe^{3+} [25,27] or due to the reduction/oxidation process induced by some quinones with the known exception of trimethyl-BQ and plastoquinone [27,28]. Either bound Q_A plastoquinone or exchangeable Q_B plastoquinone are outside the immediate coordination shell of Fe^{2+} [22] but the redox states of the quinones may influence (or be influenced by) the ligand symmetry of the non-heme iron. It is assumed that D2His215 and D1His215 are bound to quinone Q_A and Q_B through the hydrogen bonds, respectively [21]. On the other hand, it is suggested that the non-heme iron may facilitate electron transfer between the quinones and their protonation and plays a structural role in binding subunits of the reaction center complex [3,29,30]. It is known that the non-heme iron Fe^{2+} can be reversibly removed from bacterial reaction centers and replaced by other metals ions (Zn^{2+}, Co^{2+}, Ni^{2+}, Cu^{2+}, Mn^{2+}), which only moderately slow electron transfer [31]. However, it is difficult to remove non-heme iron from PSII and although there are reports on its decoupling from Q_A^- the attempts in reconstitution of photosystem II with other metals were not successful [32]. There are some discrepancies as regards to the influence of the iron depletion on the kinetics of electron transport between pheophytin and Q_A quinone [32–34]. It is not clear whether all procedures eliminating the magnetic interaction between $Q_A^{-\bullet}$ and Fe^{2+} indeed remove the non-heme iron as has been observed in PSII membrane fragments twice treated with an 'iron depletion' procedure [35] or whether only convert it to a diamagnetic state that has been detected in PSII treated with cyanides [36]. There is an interesting problem whether the diamagnetic state can occur in native systems and what alteration of the PSII function it may induce.

To gain more insight into the role of non-heme iron and cytochrome b_{559} in the electron and proton transport processes within photosystem II, it is important to know the electronic and structural properties of these two iron binding sites. EPR and Mössbauer spectroscopy have already proven to be powerful tools in such studies [22,25,28,35,36]. The Mössbauer method permits the study of diamagnetic states of Fe^{2+}, which are EPR silent. Temperature measurements of the Mössbauer recoil-free fraction yield information on lattice dynamics. Investigations of the vibrational and collective motions of the Mössbauer probe give information on local modes, which are unobtainable by other techniques. High purity of the PSII preparations and homogeneity of the sample are the most important factors in such studies.

In this work we present a thorough study of new valence and spin states of the non-heme and heme iron as well as the characterization of their collective modes in intact thylakoid membranes from a mutant of *Chlamydomonas reinhardtii* free of photosystem I (PSI^-). We have shown that both of the Fe states are able to interact with α-TQ, the role of which in photosystem II is of great interest.

2. Materials and methods

We performed our experiments on ^{57}Fe-enriched thylakoid membranes from a mutant of *C. reinhardtii* free of photosystem I (PSI^-). The PSI deficiency of strain Xba9 was caused by the disruption of a psaA exon downstream of the psbD gene. The mutation was achieved by an in vitro mutagenesis approach, using the plasmid vector pCA1 and the *aad*A-selectable marker [37] for chloroplast transformation with a gun-powder driven DNA particle-delivery instrument (Shearline-MK2, UK). Xba9 cells were cultivated in TAP medium [38] with ^{57}Fe-containing Hutner's trace solution. Thylakoid membranes were isolated according to Diner and Wollman [39] by sucrose cushion centrifugation. α-TQ was obtained as described in [40]. It was added to the sample at a TQ/Chl molar ratio of 1:10.

For immunoblotting with polyclonal anti-PetA (dilution 1:1000) and anti-PsbE (dilution 1:2000) nitrocellulose membranes were prepared and stained following the procedures of Kruse et al. [41].

Mössbauer spectra have been recorded in a gas-flow cryostat in the temperature range of 78–270 K with the 40 mCi Co/Cr source at room temperature. The temperature stabilization was within 0.1 K. The isomer shifts are given vs. metallic Fe at room temperature.

3. Results and discussion

Mössbauer spectra of thylakoid membranes recorded at temperatures below 269 K consist apparently of a symmetric quadrupole doublet with broadened lines. To evaluate these spectra in an independent way, a Gaussian distribution of quadrupole splitting was assumed. The obtained distribution clearly shows two maxima (inset in Fig. 1). Thus, it is concluded that the spectra are superpositions of two quadrupole doublets with different splitting and identical isomer shifts (Fig. 1). For further discussion they were fitted assuming just two doublets. The hyperfine parameters for these two components are presented in Fig. 2A (isomer shift) and Fig. 2B (quadrupole splitting).

The decrease of the isomer shift (or, more precisely, the central shift) with increasing temperature is due to the second-order Doppler shift, a dynamic relativistic effect. Thus, no change of electron density at the ^{57}Fe nuclei is observed. The quadrupole splittings do not change with temperature. The absorption lines are narrow (they do not exceed 0.2 mm/s). These facts indicate homogeneous surroundings of Fe with a stable electron configuration of each of the components. Immunoblotting of isolated thylakoid membrane preparations using an antibody raised against one of the subunits of the cytochrome b_6/f complex (anti-cytochrome *f*, cross-reacting with subunit IV) clearly demonstrated that Xba9 thylakoid membranes contain only very low amounts of cytochrome *f* (PetA) compared to wild type and no detectable amounts of the cytochrome b_6/f complex subunit IV (PetD). From these data an overall amount of less than 5% of cytochrome b_6/f complexes was calculated densitometrically in the PSI^- mutant compared to the wild type (Fig. 3). In addition, the hyperfine parameters of the components in our spectra are not characteristic for the cytochrome b_6/f complex [42,43]. From the discussion above it is clear that the two Mössbauer components cannot come from other iron proteins than the PSII complex. There are only two possible candidates: the non-heme iron and cytochrome b_{559}. Using Western blotting based on equal protein concentrations we calculated that the α-subunit of cytochrome b_{559} is present in Xba9 thylakoid membranes in a concentration range of about 60% compared to the wild type (Fig. 3).

The obtained hyperfine parameters exclude a Fe^{2+} high spin

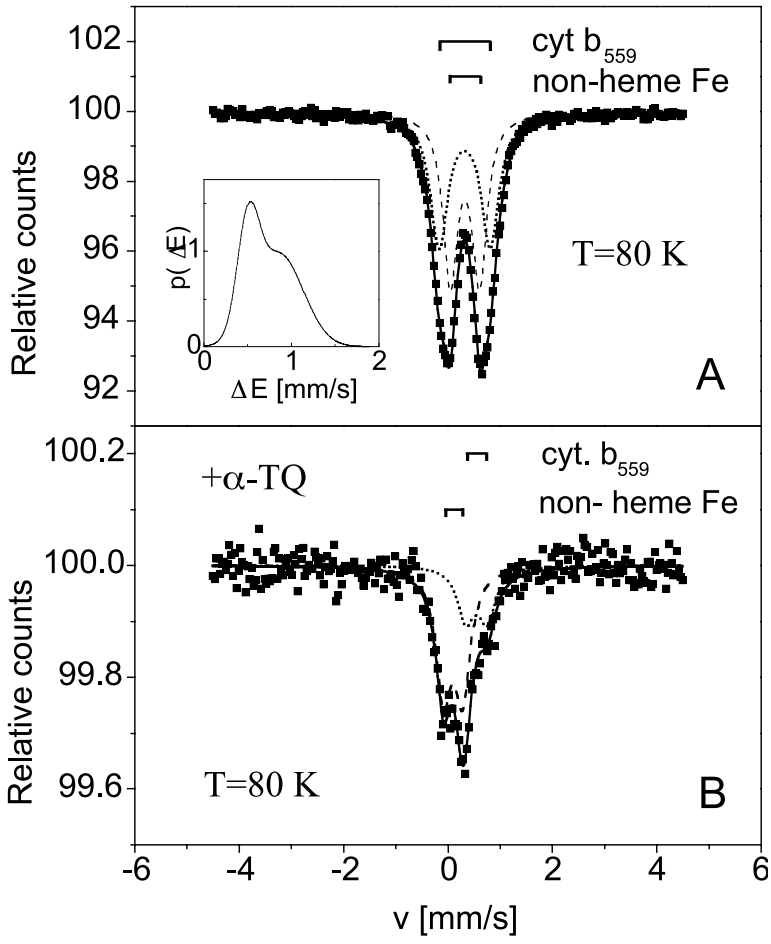

Fig. 1. ^{57}Fe Mössbauer absorption spectra of PSII thylakoid membranes isolated from the *C. reinhardtii* Xba9 PSI$^-$ mutant. A: $T = 80$ K. B: After dark incubation with α-TQ at $T = 80$ K. The lines represent theoretical fits assuming two symmetrical doublets. Subspectra correspond to the heme iron in cytochrome b_{559} and the non-heme iron. Quadrupole splitting distribution, in the case of the untreated sample, is shown in the inset in A.

state. The treatment of the thylakoids with hydroquinone and/or ascorbate did not influence the hyperfine parameters of the two iron states. This means that both of them are in the reduced form Fe^{2+} and further that only the Fe^{2+} low spin state may be assigned to both components ($\delta_1 \approx \delta_2 \approx 0.480 \pm 0.005$ mm/s and $\Delta E_1 = 1.05 \pm 0.05$ mm/s; $\Delta E_2 = 0.55 \pm 0.03$ mm/s at 80 K). There is no doubt that the component characterized by a quadrupole splitting of about 1 mm/s can be ascribed to cytochrome b_{559} [25,35,44]. The isomer shift and quadrupole splitting are characteristic for low spin Fe^{2+} heme iron in a strong ligand field [45]. Such an iron state is typical for Fe complexes with nitrogen ligands coming from a high degree of covalent overlap between the central metal atom and the ligands [46]. The value of the quadrupole splitting suggests inequivalence of the covalence between the axial and equatorial ligands leading to the tetragonal distortion of the octahedral symmetry.

It is reasonable to assign the second component to the non-heme iron. Indeed, it is unlikely that PSII thylakoids studied here can be depleted of non-heme iron because it is very difficult to remove it from the PSII membranes [32]. It should be pointed out that we did not use any detergents in the preparation procedure. The ratio of the fractions of the second and the first component is 1.2:1 (at 80 K) indicating an equimolar amount of these two iron sites. This would point to the prediction that there is one copy of non-heme iron and cytochrome b_{559} per PSII reaction center and could favor the cytochrome b_{559}:PSII stoichiometry of 1:1 which is still under debate (1:1 versus 2:1) [47,48]. Ascorbate, known to reduce non-heme iron, did not change the hyperfine parameters of this component. The arguments applied to the heme iron lead to the conclusion that non-heme iron is in a low spin ferrous state. The smaller quadrupole splitting of non-heme iron is consistent with the decreasing difference between the electron withdrawing abilities of the ligands in comparison with the plane porphyrin nitrogens and axial histidines in the case of cytochrome b_{559} [49]. The values of ΔE_2 and δ_2 can be assigned to a four- or six-coordinated Fe^{2+} in a strong ligand field. It should be stressed that we do not observe any high spin ferrous state of the non-heme iron. In order to explain the absence of the high spin ferrous state, a detailed structural analysis of the binding site in the PSI$^-$ mutant of *C. reinhardtii* is required. It is, however, possible that the non-heme Fe^{2+} iron can adopt either the high spin $^5T_2$ state in a week ligand field (usually detected) or low spin $^1A_1$ state in a strong ligand field as is observed in our case. Depending on the energies between the two states they can coexist or only one of them can be present. Such a crossover of Fe complexes dependent on temperature is well known [50]. In the case of the non-heme iron, the protein structure in its vicinity may play the

role of a temperature factor and be responsible for stabilizing one of the states or allowing coexistence of both of them and/or intermediate states. This could explain for example the appearance of more than one non-heme iron high spin component with various quadrupole splittings (the difference of ΔE is about 0.5–0.9 mm/s) [26,44] exhibiting different sensitivity to external cofactors [51].

The temperature analysis of the recoil-free fraction has allowed us to show two different environments of the absorbing nucleus. From the temperature dependence of the absorption area of the spectra, which for thin absorbers are proportional to the Lamb–Mössbauer factor $f = \exp(-k^2\langle x^2\rangle)$ (where $k = 1/0.137$ Å^{-1} is the wave number of the 14.4 keV gamma ray for ^{57}Fe), we have calculated the mean square displacement $\langle x^2\rangle$ of the two iron states. We have normalized $\langle x^2\rangle$ by its extrapolation to 0 for $T = 0$ according to the classical approach (the quantum mechanical zero point vibrations are neglected). The results are presented in Fig. 4.

The mean square displacement $\langle x^2\rangle_t$ of iron can be approximated by a sum of three statistically independent terms [52]:

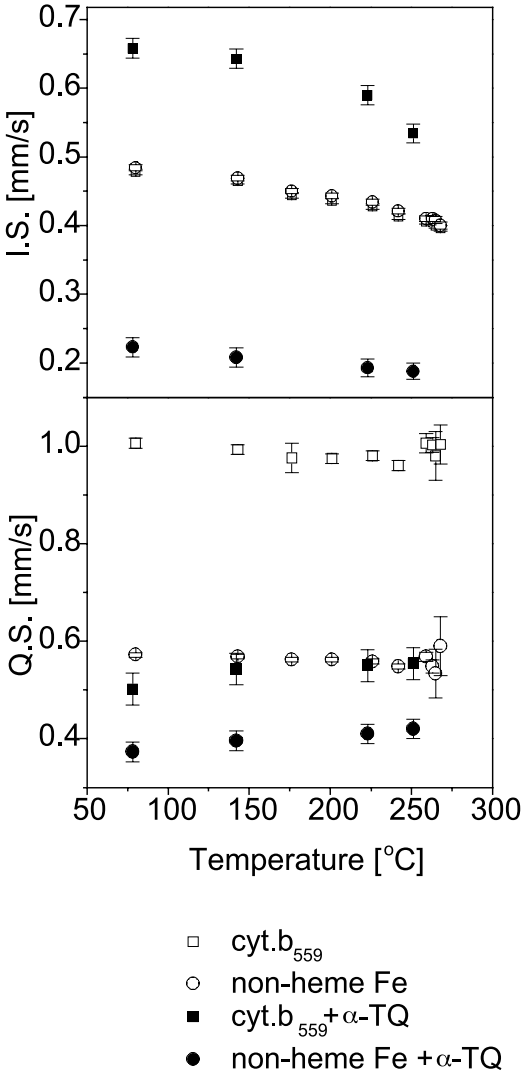

Fig. 2. The temperature dependence of isomer shifts (A) and quadrupole splittings (B) of the non-heme iron and the heme iron of cytochrome b_{559} in untreated PSII thylakoid membranes isolated from the *C. reinhardtii* Xba9 PSI$^-$ mutant and incubated with α-TQ.

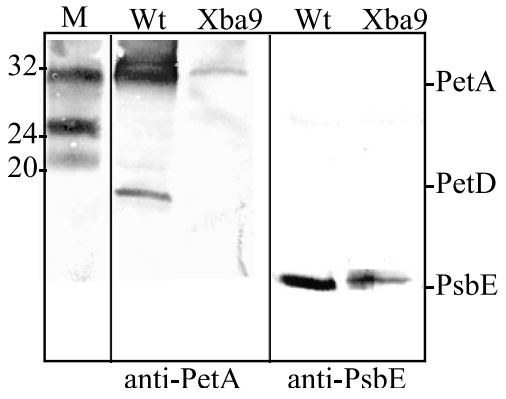

Fig. 3. Immunoblot of *C. reinhardtii* Xba9 thylakoids separated by a Tris/Tricine sodium dodecyl sulfate–polyacrylamide gel electrophoresis (SDS–PAGE) using 10% acrylamide and incubated with polyclonal anti-cytochrome *f* (PetA) and anti-α-cytochrome b_{559} (PsbE). Wt, wild type of *C. reinhardtii*.

$$\langle x^2\rangle_t = \langle x^2\rangle_v + \langle x^2\rangle_{cf} + \langle x^2\rangle_{cs}$$

where indices v, cf and cs are related to vibrational, collective fast and collective slow (diffusional) modes. Within the temperature range 78–265 K $\langle x^2\rangle_t$ is the sum of vibrational and fast collective motions (Fig. 4). The so-called bound diffusion (slow collective motions) [53] responsible for the appearance of a broad line has been detected at $T = 269$ K (Fig. 5). These motions are associated with the fluidity of the protein matrix but we will not elaborate this point here. We concentrate on the analysis of the data for $T < 269$ K. Above a characteristic temperature (> 200 K in our case and usually in large biomolecules) groups of atoms can occupy different substates according to the Boltzmann distribution but below the characteristic temperature they stay in the same substate. In the most simple case, one considers only two main substates of the resonant atom [54,55]. The energetic difference between the substates is given by E and the separation potential barrier by Q. The distance between the two substates is d. The transition rate from the higher potential well to the lower one is given by:

$$k_H = \nu_0 \exp\left(-\frac{Q}{k_B T}\right)$$

and from the lower potential well to the higher one by:

$$k_L = \nu_0 \exp\left(-\frac{E + Q - T\Delta S}{k_B T}\right)$$

where $\nu_0 = 10^{13}$ s^{-1} is a typical vibrational frequency of a solid, T is the temperature, k_B the Boltzmann constant and ΔS is the activation entropy. Assuming that $k_H \gg k_L$ one receives the following expression for $\langle x^2\rangle_{cf}$:

$$\langle x^2\rangle_{cf} = \frac{d^2 k_L}{k_H + \tau^{-1}}$$

where $\tau = 1.4 \times 10^{-7}$ s is the life-time of the excited state of Fe. The fitted parameters Q, E and d are presented in Table 1. The theoretical curves are shown in Fig. 4 (solid lines). The energetic difference between the two conformational substates and the energetic potential barrier for heme iron of cytochrome b_{559} and non-heme iron agree within the errors. They are about two times lower than those obtained for my-

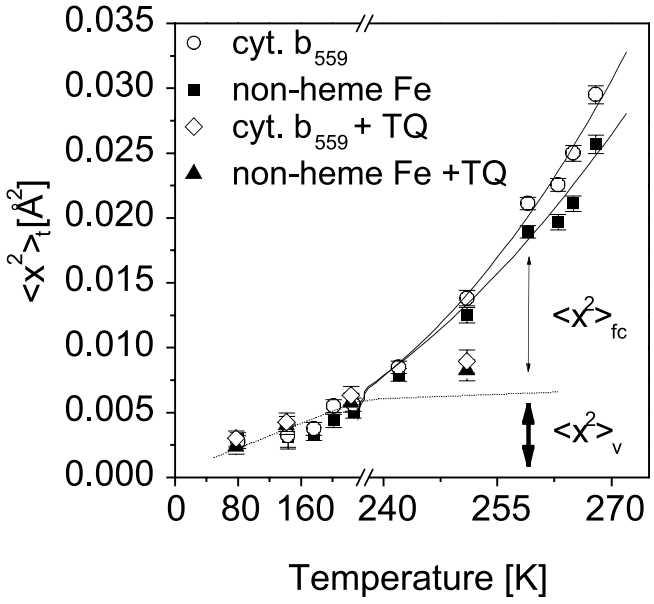

Fig. 4. Temperature dependence of the conformational $\langle x^2\rangle_{cf}$ and vibrational $\langle x^2\rangle_v$ mean square displacement for the non-heme and heme iron in PSII thylakoid membranes isolated from the *C. reinhardtii* Xba9 PSI$^-$ mutant.

oglobin[1] [54]. The determined value of Q is about four times higher than the energetic barrier estimated for chromatophore membranes from *Rhodospirillum rubrum* (3.85 kJ/mol) whereas the energetic difference between two substates is almost three times lower (9.65 kJ/mol). In this comparison, one should bear in mind that the data are for iron–sulfur centers of the photosynthetic bacterium, contributing mainly to the Mössbauer spectrum [56]. The distance between the two substates for cytochrome b_{559} is significantly higher than for non-heme iron (Table 1) and myoglobin [54] but almost two times lower than the value one finds for *R. rubrum* chromatophores [56]. The comparison of the parameters estimated for the species mentioned above indicates that both heme iron and non-heme iron in photosystem II are in more rigid surroundings than Fe–S centers in the bacterium but in a less rigid environment than heme iron in myoglobin. The same characteristic energies for the substates in the case of non-heme iron and iron in cytochrome b_{559} (Table 1) suggest that the same fast conformational motions are responsible for the collective modes for both of the iron atoms in PSII, leading, however, to the higher liberation of the heme iron. This is in agreement with the observation that either non-heme iron or heme iron in cytochrome b_{559} are exposed to the stromal side and both of them operate on the acceptor side of photosystem II [2]. The d values obtained for the two iron probes are typical for the displacement of the side chain atoms [57]. The smaller quadrupole splitting in the case of non-heme iron indicates the existence of stronger bonds within the protein matrix than it is observed for cytochrome b_{559} iron. This is consistent with the larger mean square displacement of the heme iron than of the non-heme iron (Table 1).

An independent approach describing the temperature behavior of $\langle x^2\rangle$ is the Debye model extended for anharmonicity at higher temperatures [55]. Generally, below the Debye temperature $\langle x^2\rangle$ increases linearly with temperature and one can attribute these motions to lattice or solid-state vibrations $\langle x_v^2\rangle$ (see Fig. 4). Assuming a temperature-dependent Debye temperature: $\Theta_D = \Theta_0(1+AT+\ldots)$, where Θ_0 is the Debye temperature in the low temperature limit and A is an anharmonicity parameter, we obtained Θ_0 and A for cytochrome b_{559} heme iron and non-heme iron, which are presented in Table 1. As one can expect, the Θ_0 in these cases are lower than those found for lyophilized Fe cytochrome c [55]. The Debye temperature of the non-heme iron is higher than that of the heme iron. This is again consistent with the more rigid binding site of non-heme iron than of iron in cytochrome b_{559}.

It is well known that rapid conformational fluctuations of

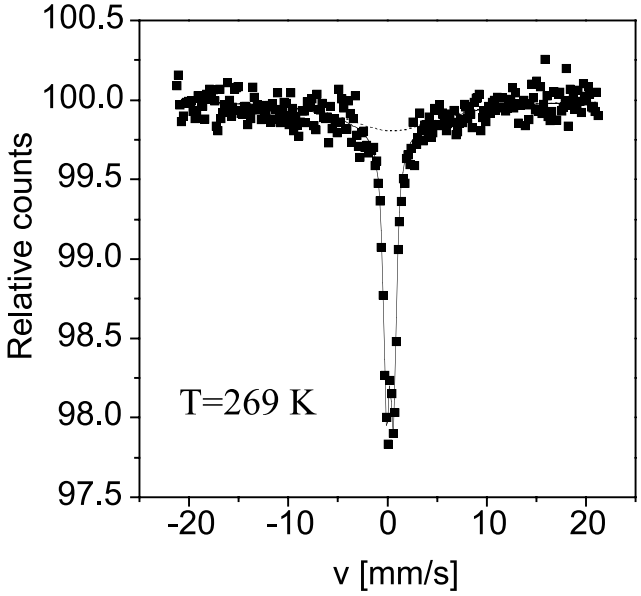

Fig. 5. ^{57}Fe Mössbauer absorption spectra of PSII thylakoid membranes isolated from the *C. reinhardtii* Xba9 PSI$^-$ mutant measured at 269 K. A single broad component corresponds to the diffusional motion of the protein matrix.

[1] Note the inversion of the E and Q parameters in the cited work.

Table 1
Experimentally determined parameters of the Debye model extended for anharmonicity (Θ_0, Debye temperature; A, anharmonicity parameter) and the double state model (E, energy difference between the two states; Q, energy barrier; d, distance)

	Θ_0 (K)	A (10^{-5} K^{-1})	Q (kJ/mol)	E (kJ/mol)	d^2 (Å^2)[a]
Cytochrome b_{559} Fe^{+2} low spin	182 ± 5	−7.0 ± 2.0	16.0 ± 1.1	3.5 ± 2.0	0.98 ± 0.20
Non-heme Fe^{+2} low spin	194 ± 6	−0.3 ± 0.1	15.0 ± 1.3	3.0 ± 1.5	0.60 ± 0.10

[a]Assuming $\Delta S = 0$.

biological macromolecules are essential for the functional properties of the systems [58]. This is also true for the case of the exchange of a platoquinone molecule at the Q_B site and of the electron transfer $Q_A^- Q_B \rightarrow Q_A Q_B^-$ [23,59]. Indeed, if one neglects conformational fluctuations and estimates free energies of the states $Q_A^- Q_B$ and $Q_A Q_B^-$ from electrostatic considerations one finds that the electron transfer is disfavored [60]. Thus, the observed electron transfer must be attributed to the presence of some dynamic effects like conformational fluctuations of the system. Now, a question arises as to what is known about these conformational fluctuations. The answer to this question is that the fluctuations are accompanied by changes in the non-heme Fe^{2+} high spin state and the ferrous state of the heme iron in cytochrome b_{559} as it was found in the studies of the electron transfer between quinones in PSII membrane fragments [61]. A similar effect has been observed for the non-heme iron in bacterial photosynthetic membranes [56].

The fact that α-TQ influences photosynthetic electron transport [62,63] and that α-TQ does not act as an electron acceptor in PSII [64] is well established. However, the mechanism of its action remains to be clarified. α-TQ inhibits electron transport changing the oxygen evolution pattern in a way which shows that the probability of a slower mode of oxygen yield increases [64–66]. It has been shown to oxidize efficiently the reduced LP form of cytochrome b_{559} in darkness but was inactive in stimulating photoreduction of the cytochrome [18]. Moreover, it has been demonstrated that TQ stimulates oxidation of the cytochrome b_{559} HP form in the dark reaction [20]. In our studies we checked the possible interaction of α-TQ with the low spin non-heme iron and cytochrome b_{559} in the PSI^- mutant. Mössbauer spectra of PSII membranes treated with α-TQ are presented in Fig. 1B. The fitted parameters are included in Fig. 2A and B. Because of the low concentration of the sample we could not perform more detailed temperature-dependent experiments (only up to 251 K). Spectra are characterized by two narrow doublets (∼0.2 mm/s), which again indicated two homogeneous iron states. The non-heme iron due to interaction with α-TQ is still in the low spin ferrous state. The hyperfine parameters of the non-heme iron after treatment with α-TQ (Fig. 2) are identical with the hyperfine parameters of the cyanide-induced low spin non-heme Fe^{2+} (isomer shift = 0.26 mm/s and quadrupole splitting = 0.36 mm/s, at 80 K) [36]. This is consistent with the expectation of stronger covalent bonds with tocopherol quinone and an increase in the π back donation to the ligand anti-bonding orbitals. On the other hand α-TQ causes oxidation of cytochrome b_{559}. The heme iron changes its state to high spin Fe^{3+}. This can be explained by a ligation of α-TQ to the iron, most probably by exchange of the distal histidine. Direct oxidation of the heme iron in the cytochrome b_{559} HP form by α-TQ is not possible because of its low redox potential ($E_{m,7} = 0$ mV) [67] but it probably oxidizes the HP form by its deprotonation [20] similar to that of FCCP [19]. Either in the case of the non-heme iron or the heme iron, α-TQ interactions result in an increase of the rigidity of their environment and increase of the Debye temperature to about 220 K.

In summary, we have observed that the non-heme iron and the heme iron of cytochrome b_{559} are in the low spin ferrous states in PSII thylakoid membranes prepared from a *C. reinhardtii* PSI^- mutant. The higher Debye temperature of non-heme iron suggests that it is in a more rigid protein environment than in the heme iron. This is in agreement with the observation that the fast collective motions at the acceptor side of photosystem II, characterized by similar potential barriers and energetic differences between the conformational substates of the two iron protein matrices, lead to a higher liberation of the heme iron in cytochrome b_{559} than in the case of the non-heme iron. We have shown that α-TQ can interact with the non-heme iron and with cytochrome b_{559}. It is very interesting to notice that cyanide and α-TQ convert non-heme iron to the same low spin ferrous state. Both compounds cause the slowing down of electron transport within PSII [51,64] resulting in a lower efficiency of the water splitting process. This is an indication for the important role of a non-heme iron in photosystem II. A direct interaction between α-TQ and cytochrome b_{559} causes the oxidation of the heme iron which is consistent with our earlier observation that tocopherol quinone can oxidize LP and HP forms of cytochrome b_{559} in the dark. The occurrence of this interaction reveals the important role of α-TQ as a regulatory component in cyclic electron flow around PSII and the protection against photoinhibition.

Acknowledgements: K.B. thanks the European Commission for IHP Marie Curie Fellowship. This work was supported partially by Grant P04A 03817 from the Committee for Scientific Research (KBN) of Poland and the Deutsche Forschungsgemeinschaft (Kr1586-2/2 and FOR387). The Xba9 *Chlamydomonas* mutant was constructed by Drs. Peter Nixon and Christos Andronis, to whom we are most grateful. The anti-cytochrome *f* was a kind gift of F.A. Wollman.

References

[1] Hankamer, B. and Barber, J. (1997) Annu. Rev. Plant Physiol. Plant Mol. Biol. 48, 641–671.
[2] Zouni, A., Witt, K.T., Kern, J., Fromme, P., Krauß, N., Saenger, W. and Otrh, P. (2001) Nature 409, 739–743.
[3] Deisenhofer, J., Epp, O., Miki, K., Huber, R. and Michel, H. (1985) Nature 318, 618–624.
[4] Stewart, D.H. and Brudvig, G.W. (1998) Biochim. Biophys. Acta 1367, 63–87.
[5] Barber, J. and De Las Rivas, J. (1993) Proc. Natl. Acad. Sci. 90, 10942–10946.
[6] Marc, J. and Garnier, J. (1981) Biochim. Biophys. Acta 637, 473–480.
[7] Parkasi, H.B., De Ciechi, P. and Whitmarsh, J. (1991) EMBO J. 10, 1619–1627.
[8] Shukla, V.K., Stanbekova, G.H., Shestakov, S.V. and Parkasi, H.B. (1992) Mol. Microbiol. 6, 947–956.
[9] Annanyev, G., Renger, G., Wecker, U. and Klimov, V. (1994) Photosynth. Res. 41, 327–338.

[10] Tae, G.S., Black, M.T., Cramer, W.A., Vallon, O. and Bogorad, L. (1988) Biochemistry 27, 9075–9080.
[11] Alizadeh, S., Nechushtai, R., Barber, J. and Nixon, P. (1994) Biochim. Biophys. Acta 1188, 439–442.
[12] Mor, T.S., Ohad, I., Hirschberg, J. and Pakrasi, H.B. (1995) Mol. Gen. Genet. 246, 600–604.
[13] Bergström, J. and Väungård, T. (1982) Biochim. Biophys. Acta 682, 452–456.
[14] Babcock, G.T., Widger, W.R., Cramer, W.A., Oerthing, W.A. and Metz, J.G. (1985) Biochemistry 24, 3638–3645.
[15] Thompson, L.K., Miller, A.F., Buser, C.A., De Paula, J.C. and Brudvig, G.W. (1989) Biochemistry 28, 8048–8056.
[16] Roncel, M., Ortega, J.M. and Losada, M. (2001) Eur. J. Biochem. 268, 4961–4968.
[17] Shuvalov, V.A. (1994) J. Bioenerg. Biomembr. 26, 619–626.
[18] Kruk, J. and Strzalka, K. (2001) J. Biol. Chem. 276, 86–91.
[19] Arnon, D.J. and Tang, G.M.S. (1988) Proc. Natl. Acad. Sci. USA 85, 9524–9528.
[20] Kruk, J., Schmid, G.H. and Strzalka, K. (2000) Plant Physiol. Biochem. 38, 271–277.
[21] Trebst, A. (1986) Z. Naturforsch. 41c, 240–245.
[22] Dismukes, G.Ch., Frank, H.A., Freiser, R. and Sauer, K. (1984) Biochim. Biphys. Acta 764, 253–271.
[23] Feher, G., McPherson, P.H., Paddock, M., Romgey, S.H., Schönfeld, M. and Okamura, M.Y. (1990) in: Current Research in Photosynthesis, Vol. I (Baltscheffsky, M., Ed.), pp. 39–46, Kluwer Academic, Dordrecht.
[24] Blubaugh, D. and Govindjee (1988) Photosynth. Res. 19, 85–128.
[25] Diner, B.A. and Petrouleas, V. (1987) Biochim. Biophys. Acta 893, 138–148.
[26] Petrouleas, V. and Diner, B.A. (1982) FEBS Lett. 147, 111–114.
[27] Petrouleas, V. and Diner, B.A. (1987) Biochim. Biophys. Acta 893, 126–137.
[28] Zimmermann, J.L. and Rutherford, A.W. (1986) Biochim. Biophys. Acta 851, 416–423.
[29] Dutton, P.L., Prince, R.C. and Tiede, D.M. (1978) Photochem. Photobiol. 28, 939–949.
[30] Xu, C., Taoka, S., Crofts, A.R. and Govindjee (1991) Biochim. Biophys. Acta 1098, 32–40.
[31] Debus, R.J., Feher, G. and Okamura, M.Y. (1986) Biochemistry 25, 2276–2287.
[32] MacMillan, F., Lendzian, F., Renger, G. and Lubitz, W. (1995) Biochemistry 34, 8144–8156.
[33] Kirmaier, C., Holten, D., Debus, R.J., Feher, G. and Okamura, M.Y. (1986) Proc. Natl. Acad. Sci. USA 83, 6407–6411.
[34] Agalidis, I., Nuijs, A.M. and Reiss-Husson, F.C. (1987) Biochim. Biophys. Acta 890, 242–250.
[35] Kurreck, J., Garbers, A., Parak, F. and Renger, G. (1997) FEBS Lett. 403, 283–286.
[36] Sanakis, Y., Petrouleas, V. and Diner, B.A. (1994) Biochemistry 33, 9922–9928.
[37] Andronis, Ch., Kruse, O., Deak, Z., Vass, I., Diner, B.A. and Nixon, J. (1998) Plant Physiol. 117, 515–524.
[38] Harris, E.H. (1989) The Chlamydomonas Sourcebook, pp. 576–577, Academic Press, San Diego, CA.
[39] Diner, B.A. and Wollman, F.A. (1980) Eur. J. Biochem. 110, 521–526.
[40] Kruk, J. (1988) Biophys. Chem. 30, 143–149.
[41] Kruse, O., Zheleva, D. and Barber, J. (1997) FEBS Lett. 408, 276–280.
[42] Schünemann, V., Trautwein, A.X., Illerhaus, J. and Haehnel, W. (1999) Biochemistry 38, 8981–8991.
[43] Illerhaus, J., Sanakis, Y., Petrouleas, V. and Haehnel, W., (1995) in: Photosynthesis from Light to Biosphere, Vol. II (Mathis, P., Ed.), pp. 551–554, Kluwer Academic, Dordrecht.
[44] Kurreck, J., Garbers, A., Reiforth, F., Andreasson, L.E., Parak, F. and Renger, G. (1996) FEBS Lett. 381, 53–57.
[45] Moss, T.H., Bearden, A.J., Bartsch, R.G. and Cusanovich, M.A. (1968) Biochemistry 7, 1583–1589.
[46] Shulman, R.G. and Sugano, S. (1965) J. Chem. Phys. 42, 39–43.
[47] Buser, C.A., Diner, B.A. and Brudvig, G.W. (1992) Biochemistry 31, 11441–11448.
[48] Kaminskaya, O., Kurreck, J., Irrgang, K.D., Renger, G. and Shuvalov, V.A. (1999) Biochemistry 38, 16223–16235.
[49] Bearden, A.J., Moss, T.M., Caughey, W.S. and Beaudreau, Ch.A. (1965) Proc. Natl. Acad. Sci. USA 53, 1246–1253.
[50] Greenwood, N.A. and Gibb, T.C. (1971) Mössbauer Spectroscopy, pp. 194–220, Chapman and Hall, London.
[51] Diner, B.A., Petrouleas, V. and Wendolski, J. (1991) Plant Physiol. 81, 423–436.
[52] Frauenfelder, H., Petsko, G.A. and Tsernoglou, T. (1979) Nature 280, 558–563.
[53] Nowik, I., Bauminger, E.R., Cohen, S.G. and Ofer, S. (1985) Phys. Rev. 31, 2291–2299.
[54] Keller, H. and Debrunner, P.G. (1980) Phys. Rev. Lett. 45, 68–71.
[55] Burda, K., Hrynkiewicz, A., Koloczek, H., Stanek, J. and Strzalka, K. (1994) Hyp. Int. 91, 891–897.
[56] Parak, F., Frolov, E.N., Kononenko, R.L., Mössbauer, V.I., Goldanskii, V.I. and Rubin, A.B. (1980) FEBS Lett. 117, 368–372.
[57] McCammon, J.A., Gelin, B.R. and Karplu, M. (1977) Nature 267, 585–590.
[58] Steigemann, W. and Weber, E. (1978) J. Mol. Biol. 127, 309–318.
[59] Stowell, M.H.B., McPhillips, T.M., Rees, D.C., Soltis, S.M., Abresh, E. and Feher, G. (1997) Science 276, 812–816.
[60] Beroza, P., Fredkin, D.R., Okamura, M.Y. and Feher, G. (1995) Biophys. J. 68, 2233–2250.
[61] Garbers, A., Reifarth, F., Kurreck, J., Renger, G. and Parak, F. (1998) Biochemistry 37, 11399–11404.
[62] Munne-Bosch, S. and Alegre, L. (2002) Crit. Rev. Plant Sci. 21, 31–57.
[63] Kruk, J. and Strzalka, K. (1995) J. Plant Physiol. 145, 405–409.
[64] Kruk, J., Burda, K., Radunz, A. and Strzalka, K. (1997) Z. Naturforsch. 52c, 766–774.
[65] Burda, K. and Schmid, G.H. (1996) Z. Naturforsch. 51c, 329–341.
[66] Burda, K. and Schmid, G.H. (2001) Biochim. Biophys. Acta 1506, 47–54.
[67] Okayama, S. (1983) in: Proceedings of the International Symposium on Photosynthetic Water Oxidation and Photosystem II Photochemistry (Inoue, Y., Murata, N., Crofts, A.R., Renger, G., Govindjee and Satoh, K., Eds.), pp. 393–400, Academic Press, New York.